Magnetic Circular Dichroism Used To Examine the Interaction of *Escherichia coli* Cytochrome *bd* with Ligands†

Vitaliy Borisov,‡ Alexander M. Arutyunyan,‡ Jeffrey P. Osborne,§ Robert B. Gennis,*,§ and Alexander A. Konstantinov‡

A. N. Belozersky Institute of Physico-Chemical Biology, Moscow State University, 119899 Moscow, Russia, and Department of Biochemistry, University of Illinois, Urbana, Illinois 61801

Received August 7, 1998; Revised Manuscript Received November 3, 1998

ABSTRACT: The interactions of the fully reduced and fully oxidized cytochrome *bd* from *E. coli* with ligands CO, NO, and CN^- have been studied by a combination of absorption and magnetic circular dichroism (MCD) spectroscopy. In the reduced cytochrome *bd*, MCD resolves individual bands due to the high-spin heme b_{595} and the low-spin heme b_{558} components of the enzyme, allowing one to separately monitor their interactions along with ligand binding to the heme *d* component. The data show that at low concentrations, the ligands bind almost exclusively to heme *d*. At high concentrations, the ligands begin to interact with the low-spin heme b_{558}. At the same time, no evidence for significant binding of the ligands to the high-spin heme b_{595} is revealed in either the reduced or the fully oxidized cytochrome *bd* complex. The data support the model [Borisov, V. B., Gennis, R. B., and Konstantinov, A. A. (1995) *Biochemistry* (*Moscow*) *60*, 231−239] according to which the two high-spin hemes *d* and b_{595} share a high-affinity ligand binding site with a capacity for only a single molecule of the ligand; i.e., there is a strong negative cooperativity with respect to ligand binding to these two hemes with cytochrome *d* having an intrinsic ligand affinity much higher than that of heme b_{595}.

The activation of molecular oxygen by the terminal oxidases of the respiratory chain is a key step in the energy metabolism of aerobic organisms. There are a great variety of terminal oxidases in bacteria, but they appear to be divided into two families of enzymes. Most of the oxidases are members of the heme/copper oxidase superfamily (*1, 2*), apparently derived from denitrificating enzymes (*3, 4*). The heme/copper oxidases have a bimetallic oxygen-reducing center containing a high-spin heme (*a*-, *b*-, or *o*-type) and a nearby copper ion. With some possible exceptions (*5, 6*), the heme/copper oxidases operate as redox-driven proton pumps and translocate two charges across the membrane per each electron transferred to oxygen.

The second family of oxidases comprises the *bd*-type quinol oxidases, widespread among prokaryotes, the most studied member being cytochrome *bd* from *Escherichia coli*. These enzymes are often important physiologically for cell growth under limited oxygen and other unfavorable (stressed) conditions (*7, 8*), and have also been shown to be necessary to prevent oxidative damage to the nitrogenase in some nitrogen-fixing bacteria (*9*−*12*). Cytochrome *bd* bears no similarity with the heme/copper oxidases. There is no sequence homology, and cytochrome *bd* does not contain copper. Also, the enzyme is relatively resistant to inhibition by CN^-, and is usually responsible for cyanide-resistant respiration observed in prokaryotes (*13*). Cytochrome *bd* does not pump protons. However, oxidation of quinol by oxygen is coupled to the release of protons from QH_2 to the outside and the uptake of protons consumed in water formation from inside the cells, a process that gives rise to a net electrogenic transmembrane translocation of one proton per electron (*14*−*17*).

Characteristics of the *bd* cytochromes as compared to other oxidases have been reviewed (*18*−*21*). Cytochrome *bd* from *E. coli* consists of two subunits with molecular masses of 47 and 53 kDa. The enzyme contains one low-spin (b_{558}) and two high-spin hemes (b_{595} and *d*). Heme b_{558} is probably the electron acceptor for quinol. When in the ferrous state, heme *d* can bind with high affinity to O_2, forming a very stable oxy complex; this heme is where the sequential reduction of dioxygen by four electrons to two molecules of water takes place. The role of heme b_{595} is not clear. It could simply transfer electrons from heme b_{558} to heme *d* (*22*), or form a second dioxygen-reactive center (*23, 24*), or cooperate with heme *d* to form a 'binuclear' oxygen-reducing center analogous to the heme/copper center of other oxidases (*25, 26*).

The mechanism of oxygen activation by cytochrome *bd* is not known to an extent comparable to the rather full picture available for that of the heme/copper oxidases. However, it is likely that the chemistry of the four-electron reduction of dioxygen to water is essentially the same. Four forms of cytochrome *bd*, differing in the state of heme *d*, have been resolved so far (*27*−*33*) that are apparently homologous to

† Supported by a grant from the National Institutes of Health (HL 16101 to R.B.G.), a Fogarty International Research Collaboration Award (TW00349 to R.B.G. and A.A.K.), the Russian Fund for Basic Research (97-04-49765 to A.A.K. and 97-04-49144 to A.M.A.), and by INTAS-RFBR (Grant 95-1259 to A.A.K.).

* To whom correspondence should be addressed. Telephone: 217-333-9075. Fax: 217-244-3186. Email: r-gennis@uiuc.edu.

‡ Moscow State University.

§ University of Illinois.

10.1021/bi981908t CCC: $18.00
Published on Web 12/19/1998

intermediates in the catalytic cycle of the heme/copper oxidases.

$$\text{reduced} \rightarrow \text{oxygenated} \rightarrow \text{ferryl}-\text{oxo} \rightarrow \text{oxidized}$$

The presence of two closely spaced metals (high-spin heme and Cu_B) in the dioxygen-reducing site of the heme/copper oxidases has often been considered to play a fundamental role in the efficient, concerted reduction of dioxygen, first to a peroxy intermediate, and then to water (*34, 35*). Alternatively, the copper atom might be an essential element of the proton pump, as suggested originally by Mitchell (*36*) [and see also (*37*), for example]. Notably, cytochrome *bd* lacks copper and does not pump protons, but it is very efficient catalytically. The turnover number of cytochrome *bd* reaches 2600 s^{-1} (electrons/s) for the *E. coli* enzyme (*38*) and 4000 s^{-1} for cytochrome *bd* from *Azotobacter vinelandii* (*39*). These values are 2−3-fold faster than turnover of the most rapid heme/copper oxidases, and, as discussed in (*39*) the enzyme may be a "perfect catalyst" as its turnover appears to approach the diffusion limit of dioxygen.

It has been speculated that the role of Cu_B in catalysis by cytochrome *bd* might be imitated by the high-spin heme b_{595}, viz., that hemes *d* and b_{595} are located in the protein very close to each other and form a binuclear dioxygen-reducing center functionally analogous to the heme/copper center in mitochondrial cytochrome *c* oxidase and related oxidases (*25*−*40*). However, this is simply based on an analogy with the heme/copper oxidases and is supported only by rather indirect arguments (*25*−*40*). As summarized in (*21, 41*), there is no indisputable evidence for proximity of hemes *d* and b_{595}. Furthermore, the absence of magnetic or anticooperative redox interactions between b_{595} and *d* rather argues against this proposal. Nevertheless, this remains an attractive model. Clearly, understanding the role of heme b_{595} in the mechanism of dioxygen reduction by cytochrome *bd* is central to understanding this unusual oxidase.

Relatively little is known about heme b_{595}. The iron in heme b_{595} is pentacoordinated, the fifth axial ligand for heme b_{595} being probably His-19 of subunit I (*42*). The redox midpoint potential of heme b_{595} (+110 mV) is intermediate between the E_m values of hemes b_{558} (+60 mV) and *d* (+230 mV), measured with pure enzyme in octyl glucoside at pH 7 (*43*). This is consistent with the model of heme b_{595} mediating electron transfer from heme b_{558} to heme *d*. However, pentacoordinated high-spin hemes in enzymes are more often directly engaged in the binding and activation of dioxygen, or another terminal electron acceptor. The participation of heme b_{595} in dioxygen activation, rather than simply mediating electron transfer to heme *d*, seems natural.

Pentacoordinate hemes usually bind to low molecular weight ligands such as carbon monoxide, nitric oxide, cyanide, and azide. Surprisingly, it is still not clear whether heme b_{595} does react with these exogenous ligands. Some of the absorption, IR[1], EPR, and MCD spectral changes of *E. coli* cytochrome *bd* induced by carbon monoxide, nitric oxide, nitrite, oxygen, and cyanide have been interpreted to indicate ligand binding with heme b_{595} (*23, 26, 40, 44*). Also spectral changes accompanying photodissociation of CO in *A. vinelandii* and *E. coli* cytochromes *bd*, particularly those observed at cryogenic temperatures, have been interpreted to indicate reaction of CO and oxygen with heme b_{595} (*24*−*47*). On the other hand, results of IR and resonance Raman spectroscopies do not reveal binding of CN^- or CO to the heme iron of heme b_{595} in the *E. coli* enzyme (*48*) except for some specific conditions (*25*). Also, binding of 1 mol of CO (*41, 49*) or NO (*47*) per mole of cytochrome *bd* complex, as well as room-temperature flash-photolysis/recombination studies of the CO adduct of the *E. coli* cytochrome *bd* (*33*), does not support binding of this ligand with b_{595}. It cannot be excluded that cytochromes *bd* from different species (for instance, *E. coli* and *A. vinelandii*) may behave differently in this respect.

Magnetic circular dichroism (MCD) spectroscopy has proved highly useful in the studies of hemoproteins and, in particular, of the respiratory chain cytochromes [reviewed (*50, 51*)]. Since the first report on the MCD spectra of the mitochondrial respiratory chain membrane-bound cytochromes (*52*), MCD characteristics of the mitochondrial aa_3-type cytochrome *c* oxidase (*53*−*57*) and of the *E. coli* bo_3-type ubiquinol oxidase (*58*−*60*) have been studied in significant detail. In contrast, MCD characteristics of cytochrome *bd* have not been explored except for two brief reports on the MCD spectra of the air-oxidized enzyme (*26, 61*).

In this work, room-temperature MCD in combination with conventional absorption difference spectroscopy has been used to probe b_{595} reactivity toward exogenous ligands. The MCD is particularly useful as it allows one to observe separate signals of the low-spin b_{558} and high-spin b_{595} in the reduced cytochrome *bd*, whereas the ligand-induced absorption changes of the two chromophores are expected to overlap very significantly. The distinct MCD responses of the different hemes render it possible to specifically and quantitatively monitor the ligand interactions with heme b_{595}. In either the reduced or the oxidized state, only a small fraction of heme b_{595}, if any, reacts with the ligands such as CO, NO, or CN^- when they are present at low concentrations. Meanwhile, at high concentrations, the ligands react with the low-spin heme b_{558}, which explains some of the ligand-induced absorption changes of cytochrome *bd* attributed earlier to heme b_{595}. The results have been reported in a preliminary form at the 9th and 10th EBEC Meetings (*62, 63*).

MATERIALS AND METHODS

E. coli strain GO105/pTK1, lacking cytochrome bo_3 and overexpressing cytochrome *bd*, has been used (*64*) as the source of the enzyme. Isolation of the cytochrome *bd* complex was performed as described previously (*65*). The concentration of cytochrome *bd* has been determined from the dithionite-reduced *minus* air-oxidized difference absorption spectra using the value of $\Delta\epsilon_{628-607} = 10.8\ mM^{-1}\ cm^{-1}$ that corresponds to $\Delta\epsilon_{561-580} = 21\ mM^{-1}\ cm^{-1}$ in (*40*).

To convert cytochrome *bd* to the fully oxidized state, the enzyme was treated with the lipophilic electron acceptor $BQCl_4$ as described earlier (*66*). Absorption changes were measured in an Aminco-SLM DW 2000 UV−Vis spectro-

[1] Abbreviations: CHES, 2-(*N*-Cyclohexylamino)ethanesulfonic acid; EDTA, ethylenediaminetetraacetate; HEPES, *N*-(2-hydroxyethyl)piperazine-N′-2-ethanesulfonic acid; MCD, magnetic circular dichroism; IR, infrared; EPR, electron paramagnetic resonance; $BQCl_4$, tetrachloro-1,4-benzoquinone.

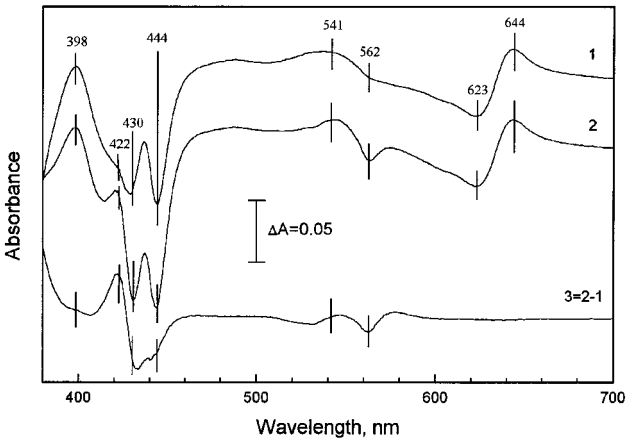

FIGURE 1: Difference absorption spectra induced by the interaction of the purified dithionite-reduced cytochrome *bd* with carbon monoxide (i.e., the spectrum of CO−ferrous cytochrome *bd* minus the spectrum of ferrous cytochrome *bd*). Curve 1, effect of 20 μM CO. Curve 2, effect of 1 mM CO. Curve 3, 1 mM CO minus 20 μM CO. The sample cell contains 4.3 μM cytochrome *bd* in 50 mM HEPES/50 mM CHES buffer, pH 8.0, and 0.025% sodium *N*-lauroylsarcosinate.

photometer. Magnetic circular dichroism spectra were monitored at room temperature with a computer-controlled dichrograph equipped with an electromagnet (effective magnetic field ~0.7 T for a 1 cm cell) constructed by Dr. A. Arutyunyan in the A. N. Belozersky Institute (Moscow State University). The instrument was calibrated as described (*50*). For each MCD spectrum reported, the spectra recorded in the direct and reverse magnetic field directions have been subtracted from each other to eliminate the contribution due to circular dirchroism. Processing and simulation of the MCD spectra were performed with the aid of graphic programs RDA and WTEST developed by I. Khomenkov and A. M. Arutyunyan in the A. N. Belozersky Institute. In some cases, the data were processed using a software package GIM (Graphic Interactive Management) developed by Alexander Drachev in this laboratory and imported into Origin 4.00 and/or Lotus Freelance Graphic PC programs for preparation of the figures.

RESULTS

Interaction of Reduced Cytochrome bd with Carbon Monoxide and Nitric Oxide. Figure 1 shows the optical absorption changes induced by the addition of CO to the reduced purified cytochrome *bd*. The effect of CO depends on the concentration of the ligand. At low concentrations (20 μM), CO brings about (i) a red shift of an absorption band in the near-IR region with the difference absorption spectrum with λ_{max} = 644 nm and λ_{min} = 623 nm; (ii) a broad maximum at ~541 nm; and (iii) a characteristic asymmetric W-shaped trough with minima at 430 and 444 nm in the Soret.

The absorption changes induced by CO in the near-IR range (600−700 nm) are assigned conventionally to a red shift of the ferrous heme *d* peak at 628 nm induced by addition of the ligand to the heme *d* iron. The increased absorption around 540 nm correlates with the behavior of the 628 nm band and very likely also reports changes of the absorption of heme *d*. The line shape of the difference spectrum in the Soret band is unusually complex. It is not fully understood and has been proposed to report CO binding with both heme *d* and heme b_{595} (*18*, *19*).

Increasing the CO concentration to 1 mM results in additional optical absorption changes in the Soret and around 560 nm (Figure 1, spectrum 2). The difference between the absorption changes induced by high and low CO concentrations is shown by spectrum 3. In the Soret, the difference spectrum reveals a derivative-type line shape (a maximum at 422 nm, a minimum at 434 nm with a shoulder at 440 nm and a zero-crossing point around 428−430 nm) that may correspond to a blue shift of an asymmetric band centered at about 430 nm. In the visible, there is a trough at about 561 nm with local maxima both on the red and on the blue sides of the trough. In addition, there is a second minor trough at about 531 nm. Notably, there are no additional changes in the 600−700 nm region of the spectrum, showing that changes of heme *d* are fully saturated at low concentrations of CO. In general, the additional spectroscopic perturbations induced by 1 mM CO indicate interaction(s) with heme(s) *b*. The line shape of the changes around 560 nm resembles broadening of the heme(s) *b* α-band, and the Soret band changes are also consistent with a shift of the ferrous heme(s) *b* band(s) expected to center around 430 nm. The absorption changes induced by high and low concentrations of the ligand are in qualitative agreement with previously published data (*49*, *67*, *68*).

To better understand the nature of the optical changes induced by the binding of CO to the reduced cytochrome *bd*, MCD spectra of the enzyme have been studied. An MCD spectrum of fully reduced cytochrome *bd* is shown in Figure 2 (spectra 1, solid lines). The spectrum shows three basic features: (i) A small negative band at about 600 nm (Figure 2B). The position and size of this negative band are typical of a high-spin pentacoordinate ferrous heme *b* (*50*, *51*) [see also Table 1 in (*69*)]. Therefore, this signal is assigned to reduced heme b_{595}. (ii) A narrow, intensive derivative-shaped *A*-term signal centered at 560.7 nm with λ_{max} = 558 nm and λ_{min} = 564 nm, accompanied by well-resolved vibronic structure in the 500−555 nm wavelength range (Figure 2B). Such a line shape of an MCD spectrum is typical of low-spin ferrous heme proteins and model compounds with two strong axial ligands such as His/His as in cytochrome b_5 or His/Met as in cytochrome *c* (*70*−*72*). The spectrum is similar to that of the low-spin heme *b* in the bo_3 (*58*) and ba_3 quinol oxidases (*73*) and can be assigned unambiguously to the Q_{00}-band (α-band) of the low-spin ferrous heme b_{558}. The peak-to-trough molar intensity of the signal (about 400 M^{-1} cm^{-1} T^{-1}) is intermediate between those of ferrous cytochrome b_5 [370 M^{-1} cm^{-1} T^{-1} (*74*)] and cytochromes *c* [600 M^{-1} cm^{-1} T^{-1} (*72*)]. (iii) In the Soret band, an intensive asymmetric signal is observed with a positive extremum at 437 nm and two minor minima at 410 and 449 nm (Figure 2A). In general, this signal can include contributions from each of the three heme centers of the cytochrome complex, although the contribution from heme *d* is not expected to be high (*75*, *76*). An attempt was made to model the spectrum as a sum of the high- and low-spin hemes *b* using the line shapes of the MCD curves of the ferrous horseradish peroxidase (*50*) and cytochrome *c* (*72*) for the high- and low-spin components, respectively (with an appropriate wavelength shift in case of cytochrome *c*). Only an approximate fit could be attained, leaving a considerable residual broad

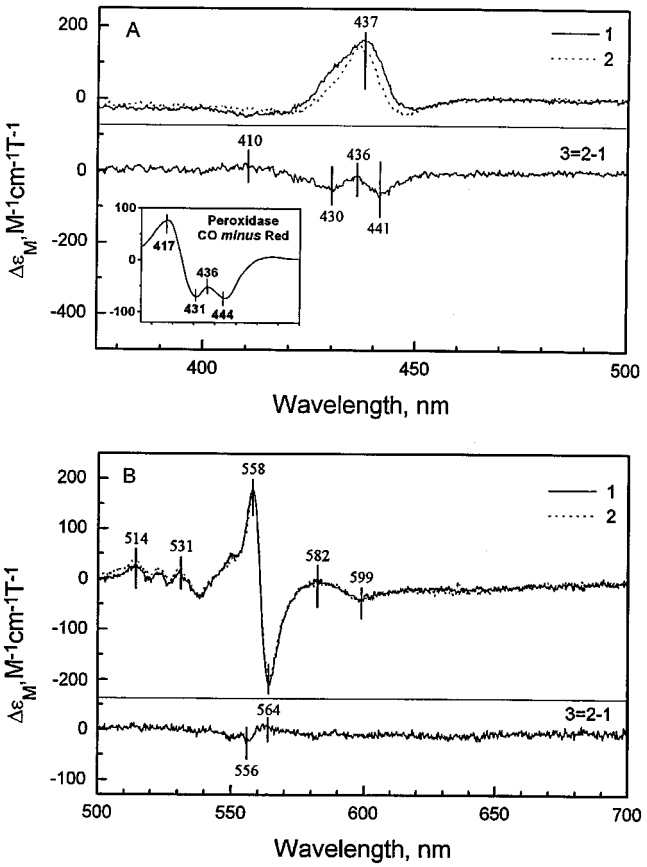

FIGURE 2: Effect of low concentrations of CO on the MCD spectrum of the reduced cytochrome *bd* in the Soret (A) and visible (B) regions. Spectrum 1 (solid line), dithionite-reduced cytochrome *bd*. Spectrum 2 (dashed line), after addition of 20 μM CO. Curve 3, difference MCD spectrum of the CO-induced changes (spectrum 2 minus spectrum 1). Other conditions as in Figure 1. Inset: MCD difference spectrum for CO binding with horseradish peroxidase (CO−ferrous peroxidase minus ferrous peroxidase) (*50*).

signal (roughly, 10−20% of the total). This residual signal is not likely to originate solely in the differences in the line shapes of the model hemoprotein MCD curves with those of hemes b_{595} and b_{558} . Rather, this is at least partly due to a weak contribution from the high-spin heme *d*, as also evidenced by the effects of the ligands (see below).

The MCD spectrum of the reduced cytochrome *bd* observed after the addition of 20 μM CO (Figure 2, curve 3, dotted lines) shows the spectroscopic changes induced by the ligand. The ligand does not affect to any measurable extent the band at 600 nm due to high-spin heme b_{595}. Also, the amplitude of the low-spin heme b_{558} signal is not decreased significantly (less than 5%). On the other hand, rather significant changes are observed in the Soret band. The signal becomes more narrow, and the difference MCD spectrum shows a W-shaped trough with minima on both sides of the center of the curve.

One possibility to consider is that these changes in the Soret might be due to the disappearance of a signal from high-spin heme *b* along with the concomitant appearance of its low-spin carbon monoxide derivative. Both of these states are expected to contribute to the MCD in the Soret. A qualitatively similar difference MCD spectrum with two minima at 431 and 444 nm is observed for CO binding with ferrous horseradish peroxidase (Figure 2A, inset). More quantitative consideration of the MCD difference spectrum of cytochrome *bd*, however, suggests that this is not an adequate explanation. The size of the trough at 441 nm, if it were due solely to CO binding with heme b_{595}, would correspond to the disappearance and conversion to the low-spin CO complex of ~25% of the high-spin ferrous b_{595}, using the CO complex of horseradish peroxidase as the model (*50*). Such an effect should be accompanied by a 25% decrease in the negative band at 600 nm. However, the latter does not decrease by more than 5%. Furthermore, there are noticeable line shape differences between the CO-induced difference MCD spectra of cytochrome *bd* and peroxidase. In particular, a prominent positive extremum at about 417 nm (Figure 2A, inset) is very weak in the difference MCD spectrum of cytochrome *bd* (Figure 2A). The size and position of the trough at 431 nm are consistent with the disappearance of the asymmetric inverted-sign signal from high-spin pentacoordinate heme *d* with an ϵ_M of 50−100 M^{-1} cm^{-1} T^{-1} (*75, 76*), provided that CO binding converts ferrous heme *d* to the low-spin hexacoordinate state [but cf. (*42, 77*)] that is likely to have very low MCD intensity in the Soret (*75, 76*).

Hence, it is suggested that the major contributions to the MCD changes in cytochrome *bd* induced by low (20 μM) CO are due to a direct interaction of the ligand with heme *d* plus, possibly, a perturbation of the heme *b* spectra induced by CO binding with heme *d*.

The MCD spectra observed at a high concentration (1 mM) of CO are shown in Figure 3. Most notably, the negative band arising from the high-spin heme *b* at 600 nm remains unchanged, whereas the *A*-term signal of the low-spin heme b_{558} diminishes by about 15% (Figure 3B). In the Soret (Figure 3A), there are only small additional changes as compared to the changes due to 20 μM CO. The trough at 429 nm becomes more pronounced while the minimum at 442 nm remains essentially unchanged. These additional changes in the Soret induced by 1 mM CO (a minimum at about 430 nm and a maximum at about 417 nm) are likely to originate in a small increase in the MCD of the CO complex of heme b_{558}.

Nitric oxide is another typical ligand of ferrous high-spin hemes. Figures 4 and 5 show the difference absorption and MCD spectra, respectively, due to the addition of 50 μM NO to reduced cytochrome *bd*. Both the absorption and MCD changes are similar to those induced by low concentrations of CO. The interesting difference consists of the absence of the "bump" at ~540 nm in the NO-induced absorption difference spectrum. The same difference can be clearly seen in the *A. vinelandii* cytochrome *bd* spectra [cf. Figures 4 and 6 in (*41*)]. Once again, there is no discernible reaction of the high-spin heme b_{595} with the ligand, as evidenced by the stability of the 600 nm negative MCD signal. In the Soret band of the MCD, the same W-shaped difference spectrum is induced as observed with CO. Experiments with high concentrations of NO were not successful due to partial precipitation of the enzyme accompanied by the complete disappearance of the low-spin *A*-term signal of heme b_{558}. This is at variance with the observations of Hori et al. (*44*), who reported that high concentrations of NO do not react with heme b_{558}, but induce full ligation of b_{595} after sufficiently long incubation.

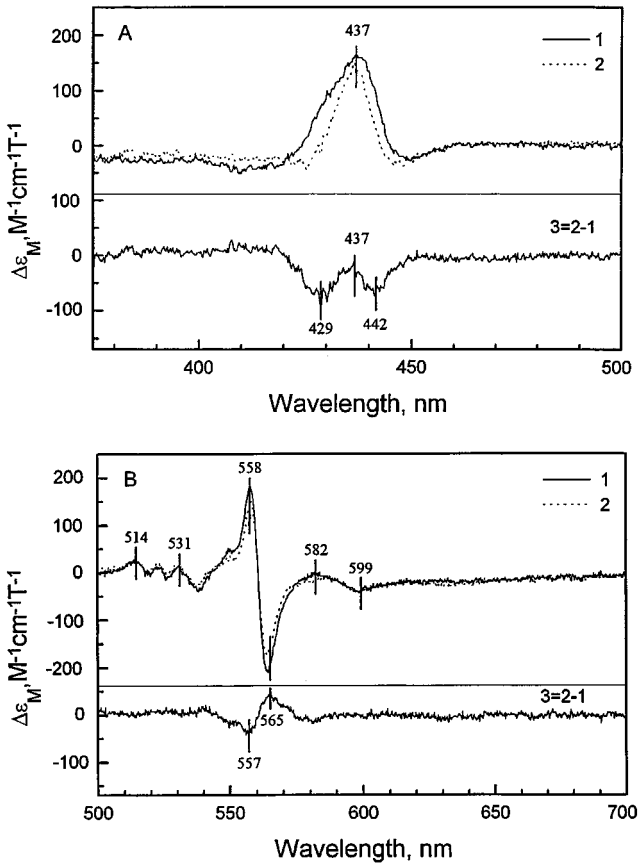

FIGURE 3: Effect of high concentrations of CO on the MCD spectrum of the reduced cytochrome *bd* in the Soret (A) and visible (B) regions. Spectrum 1 (solid line), dithionite-reduced cytochrome *bd*. Spectrum 2 (dashed line), dithionite-reduced cytochrome *bd* in the presence of 1 mM CO. Curve 3, difference MCD spectrum of the CO− induced changes (spectrum 2 minus spectrum 1). Other conditions as in Figure 1.

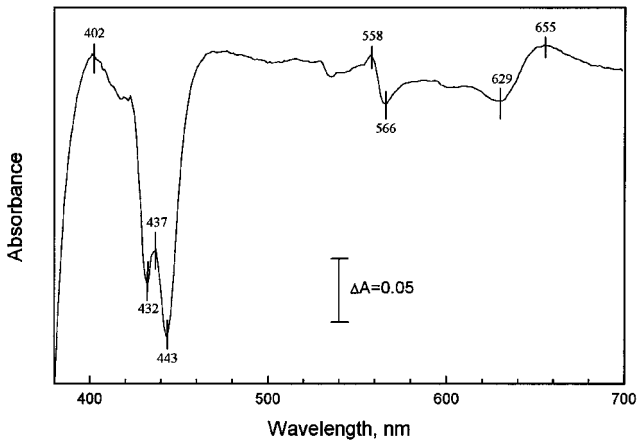

FIGURE 4: Difference absorption spectrum induced by reaction of the purified dithionite-reduced cytochrome *bd* with nitric oxide (50 μM) (NO−ferrous cytochrome *bd* minus ferrous cytochrome *bd*). Basic conditions, as in Figure 1, but the cytochrome *bd* concentration is 6 μM.

Interaction of the Oxidized Cytochrome bd with CN⁻. Most previous studies on the reaction of oxidized cytochrome *bd* with exogenous ligands were hampered by difficulties in conversion of the enzyme into the fully oxidized state. Traditional oxidants such as ferricyanide or persulfate are not efficient with cytochrome *bd*, and it is clear that many of the previous experiments with the "oxidized" enzyme

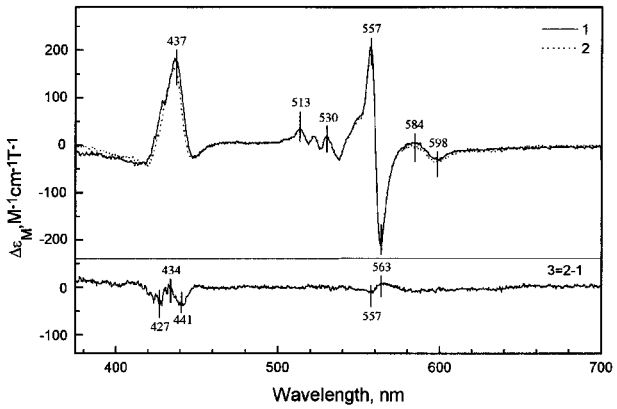

FIGURE 5: Effect of nitric oxide on the MCD characteristics of the dithionite-reduced cytochrome *bd*. Spectrum 1 (solid line), dithionite-reduced cytochrome *bd*. Spectrum 2 (dashed line), after addition of 50 μM NO to dithionite-reduced cytochrome *bd*. Curve 3, difference MCD spectrum of the NO-induced changes (NO−ferrous cytochrome *bd* minus ferrous cytochrome *bd*). The concentration of cytochrome *bd* was 6 μM. Other conditions as in Figure 1.

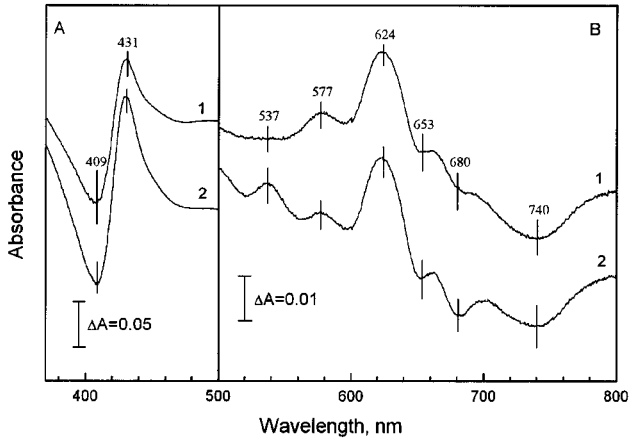

FIGURE 6: Absorption changes induced by binding of CN^- with the purified fully oxidized cytochrome *bd* in the Soret (A) and visible (B) regions (CN^-−ferric cytochrome *bd* minus ferric cytochrome *bd*). Cytochrome *bd* (5.7 μM) has been preincubated for 5 min with 80 μM $BQCl_4$ for full oxidation. Difference spectra were recorded 30 min after the addition of 0.5 mM KCN (curve 1) or 10 min after the addition of 50 mM KCN (curve 2). Other conditions as in Figure 1.

dealt, in fact, with the stable oxygenated state (oxy−ferrous complex) of the cytochrome. In this work, we have used $BQCl_4$ treatment to convert cytochrome *bd* to the all-ferric state (*66*).

The optical absorption changes induced by low and high concentrations of CN^- added to the oxidized cytochrome *bd* are shown in Figure 6. In the Soret region (panel A), CN^- induces a shift of the enzyme γ-absorption band (a derivative-shaped difference spectrum with $\lambda_{max/min}$ at 431/409 nm). In the visible/near-IR range (panel B), the major features are the peak at 624 nm, assigned provisionally to the cyano-adduct of ferric heme *d*, and the trough at 740 nm, due to the disappearance of a charge-transfer band of the ferric high-spin heme *d*. A local minimum at 680 nm is likely due to the disappearance of a small amount of contaminating ferryl−oxo form present in the oxidized sample (*78*).

Figure 7 shows the MCD spectra of cytochrome *bd* in the oxidized state (curve 1) and after addition of 0.5 mM CN^-

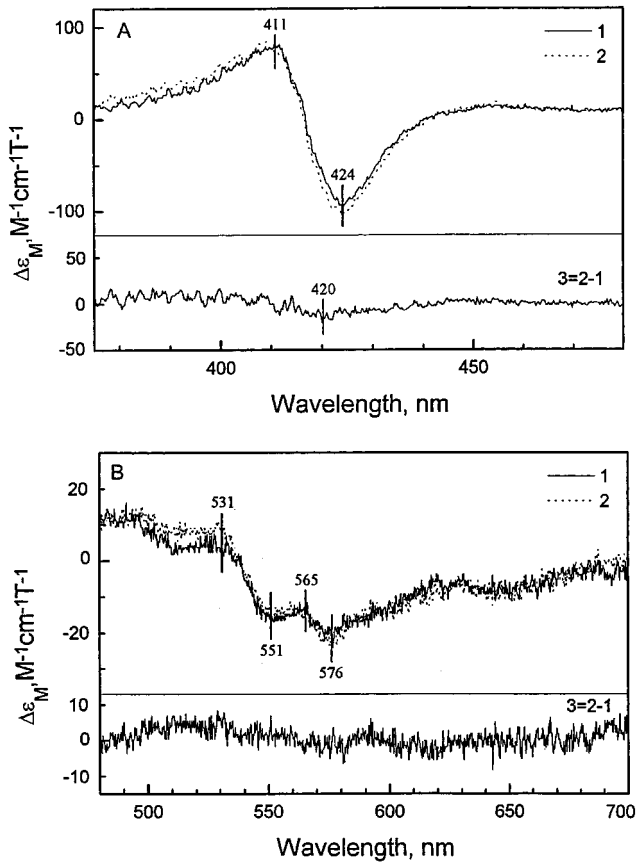

FIGURE 7: Effect of low concentrations of CN^- on the MCD spectrum of the oxidized cytochrome *bd* in the Soret (A) and visible (B) regions (CN^-−ferric cytochrome *bd* minus ferric cytochrome *bd*). Basic conditions, as in Figure 1, but the concentration of cytochrome *bd* was 5.7 μM. Spectrum 1 (solid line), oxidized cytochrome *bd* (5 min incubation with 80 μM $BQCl_4$). Spectrum 2 (dashed line), recorded 30 min after addition of 0.5 mM KCN. Curve 3, difference MCD spectrum of the KCN-induced changes (CN^-−ferric cytochrome *bd* minus ferric cytochrome *bd*).

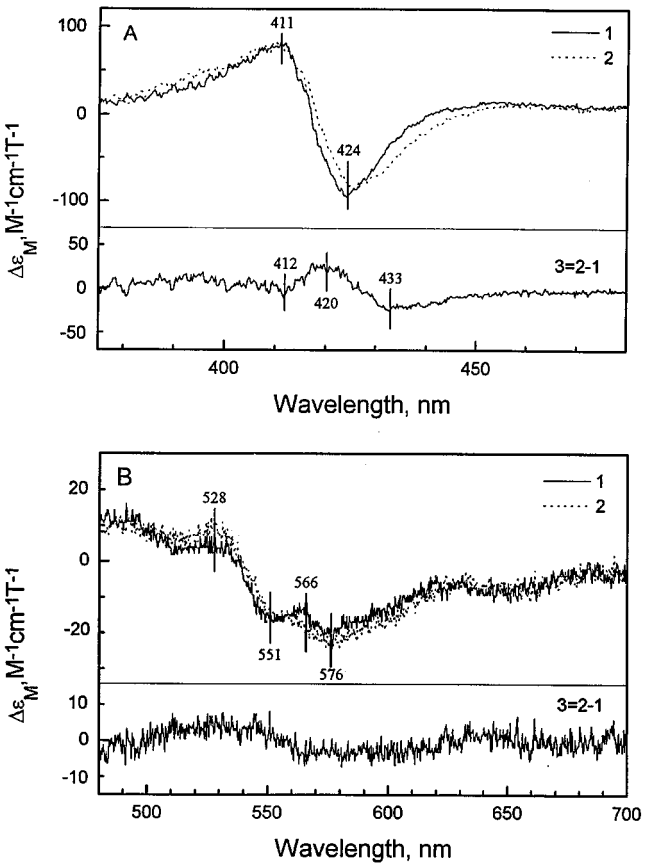

FIGURE 8: Effect of high concentrations of CN^- on the MCD spectrum of the oxidized cytochrome *bd* in the Soret (A) and visible (B) regions. Basic conditions, as in Figure 1, but the concentration of cyt *bd* was 5.7 μM. Spectrum 1 (solid line), oxidized cytochrome *bd* (5 min incubation with 80 μM $BQCl_4$). Spectrum 2 (dashed line), recorded 10 min after the addition of 50 mM KCN. Curve 3, difference MCD spectrum of the KCN-induced changes (CN^-−ferric cytochrome *bd* minus ferric cytochrome *bd*).

(curve 2). In agreement with the data in (*26*, *61*), the MCD spectrum of the oxidized cytochrome is dominated in the Soret band (Figure 7A) by a derivative-shaped signal typical of low-spin ferric heme with λ_{max} = 411 nm, λ_{min} = 424 nm, and the zero-crossing point at 417 nm. The amplitude of the signal (180 M^{-1} cm^{-1} T^{-1}) is consistent with the presence of one low-spin heme per cytochrome *bd* complex. By comparison, Soret band values of 160 and 170 M^{-1} cm^{-1} T^{-1} have been reported for the room-temperature MCD spectra of low-spin ferricytochromes *c* (*72*) and b_5 (*70*), respectively. The signal in cytochrome *bd* is most likely due to low-spin ferric heme b_{558}. High-spin ferric hemes b_{595} and *d* are not expected to contribute significantly to the MCD of the oxidized cytochrome *bd* complex. In the visible (Figure 7B), the room-temperature MCD spectrum of cytochrome *bd* shows a number of broad bands that cannot be unambiguously assigned at this time.

At relatively low concentrations (0.5 mM) of CN^-, there are virtually no changes observed in the visible range of the MCD spectrum (Figure 7B), and only very small changes in the Soret band (Figure 7A) (ca. 5% decrease of the amplitude without change at the extrema position). This small effect is incompatible with CN^- binding under these conditions to any significant fraction of heme *b* and likely originates from an interaction of the ligand with heme *d* [cf. (*75*)].

High concentrations of CN^- (50 mM) bring about more significant changes in the MCD and optical absorbance spectra in the Soret (Figures 6 and 8A). The MCD signal decreases in magnitude, and the minimum shifts by 2.5 nm to the red. These changes, as well as the corresponding MCD difference spectrum with a peak at 420 nm and troughs at 412 and 433 nm (Figure 8A), are consistent with the conversion of 15−17% of the low-spin heme b_{558} (His−Fe−Met) to the low-spin CN^- complex (His-Fe−CN^-). A contribution of a small fraction (<5%) of the high-spin heme *b* interacting with CN^- cannot be excluded.

DISCUSSION

There has been a considerable controversy accumulated in the literature concerning the ligand reactivity of the *b*-type hemes in cytochrome *bd*. Optical absorption studies have been generally interpreted to indicate interactions of heme b_{595} with CO, NO, cyanide, and some other ligands. On the other hand, the more direct spectroscopic approaches, such as resonance Raman spectroscopy, have failed to reveal coordination of cyanide at the sixth axial position of heme b_{595}, posing a question as to the validity of earlier conclusions

on the binding of other ligands with this iron−porphyrin group. The picture is clarified by the parallel MCD and absorption difference spectroscopy studies described in the current work. These studies show that, at room temperature, none of the ligands tested (CO, NO, CN^-) reacts to a significant extent with the high-spin heme b_{595} and that some of the absorption changes assigned earlier to b_{595} ligation are actually due to ligand binding with the low-spin heme b_{558}. In addition, data here and in the literature indicate a very minor perturbation of the Soret absorption band of heme b_{595} resulting from interactions of the enzyme with CO and NO, even at micromolar concentrations of the ligands. This perturbation may report two different effects. First, there might be a small red shift of the γ-band of heme b_{595} induced by ligand binding to heme *d*. Such an effect may point to heme−heme interactions between heme b_{595} and heme *d*, and thus indicate the proximity of the two iron−porphyrin groups. Second, direct binding of the ligands with heme b_{595} cannot be excluded, but this would represent only a very small fraction (5% or less) of the enzyme.

There is a very clear difference between the results showing the lack of substantial ligand interactions with heme b_{595} at room temperature and the data obtained at low cryogenic temperatures that indicate photodissociation of CO from a very significant fraction of heme b_{595} in cytochrome *bd* from both *E. coli* and *A. vinelandii*. As described below, a provisional model assuming anticooperative interactions between hemes b_{595} and *d*, proposed earlier (*79*), can reconcile most of the data and account for the unusual behavior of cytochrome *bd* interactions with ligands.

Resolution of the Signals from the Two b-Type Hemes. Spin States of the Cytochromes. The MCD spectra of reduced cytochrome *bd* reveal contributions of two hemes *b*, one low-spin and one high-spin, present at about equimolar amounts. The low-spin hexacoordinated state of heme b_{558} and the high-spin pentacoordinated state of heme b_{595} in reduced cytochrome *bd* have been inferred earlier from resonance Raman spectroscopy studies (*42*). It is important that, whereas the absorption spectra of the ferrous hemes b_{558} and b_{595} overlap significantly, the MCD characteristics of these redox centers are very different. In the visible region, MCD resolves the sharp *A*-term signal from the low-spin heme b_{558} centered at 560.7 nm and the negative lobe at 600 nm due to the high-spin heme b_{595}. In addition, the low- and high-spin hemes *b* contribute very differently to the positive Soret band signal centered at 437 nm. Hence, one can monitor the redox and spin states of these redox centers individually.

The contribution of heme *d* to the MCD spectrum appears to be small, in agreement with the low magnetooptical activity of model iron−chlorin complexes (*76*) or chlorin-reconstituted hemoproteins (*75*). The "invisibility" of heme *d* in the Soret MCD correlates with its relatively weak contribution to the absorption in this region. The heme *d* Soret absorption band is believed to be about 2−3-fold smaller than those of the hemes *b*, and, furthermore, the absorption band is rather broad [cf. hemochromogen spectra in (*44*)]. Accordingly, the shifts of the Soret band position induced by ligand binding (typically, less than 10−15 nm), that will result in diagnostic derivative-like difference spectra in case of the sharp bands of the *b* hemes, may produce rather featureless difference spectra with heme *d*. Nevertheless, it appears that ferrous high-spin heme *d* may contribute slightly to the MCD in the Soret band of the reduced cytochrome *bd*, as evidenced by the effects of CO and NO at low concentrations of the ligands.

In the visible range, the well-developed absorption band of ferrous heme *d* at about 630 nm (referred to sometimes as the "α-band") does not correlate with significant ligand- or redox-sensitive MCD changes. The absence of intensive *A*-term MCD signals associated with this band in the CO and NO complexes of heme *d* is in agreement with very low MCD signals observed for the Q_{00} band of ferrous low-spin iron−chlorins and iron−chlorin−reconstituted proteins by Dawson and collaborators (*75, 76, 80*). Most probably, this band originates from an individual Q_{0y} transition that can only give rise to a relatively weak *B*-term MCD signal. Due to the lowered macrocycle symmetry in chlorins (e.g., heme *d*), the individual Q_{0y} and Q_{0x} electronic transitions of heme *d* are expected to diverge significantly. It has been mentioned, also, that the binding of strong exogenous ligands to heme *d* iron may not convert it to the hexacoordinate low-spin state (*42*) as typical of most other hemoproteins. It is, therefore, possible that the CO and NO complexes of ferrous heme *d* remain high-spin pentacoordinate and, thus, are not expected to give strong Q_{00} band MCD signals.

The MCD characteristics of the oxidized cytochrome *bd* agree with the data in (*26, 61*), and are dominated by a low-spin ferric heme signal in the Soret. There are also some weak features in the visible that are difficult to attribute at this time. The presence of one low-spin heme in the oxidized cytochrome *bd*, corresponding to heme b_{558}, is in agreement with the EPR and resonance Raman data (*48*). Contributions of the high-spin b_{595} and *d* are not observed in the MCD, as expected for high-spin ferric species.

Heme b_{595} Does Not Bind Ligands at Room Temperature. The most important observation of this work is that the room-temperature experiments provide no evidence for any substantial interaction of heme b_{595} with exogenous ligands. Failure of heme b_{595} to bind CN^- in either the reduced or the oxidized state has also been noted in recent resonance Raman studies (*42, 48*). It cannot be fully excluded that ligand binding by heme b_{595} is simply not associated with any significant MCD or absorption changes. However, the absence of such MCD or absorbance changes would probably require that binding of the exogenous ligand displaces the axial histidine ligand such that the heme remains high-spin. Although a similar model has been considered, for instance, to explain the peculiarities with respect to ligand binding to heme *d* (*42, 77*), a simpler and far less exotic interpretation is possible to explain the observations concerning heme b_{595}.

Oxidized heme b_{595} does not interact with CN^-. In 1993 (*26*), we reported that when CN^- is added to aerobically oxidized cytochrome *bd*, the ligand binds not only to heme *d* but also to a significant part of heme *b* in the cytochrome complex. This finding was corroborated by the subsequent IR/EPR studies of Tsubaki et al. (*40*). At that time, we assigned some of the observed spectroscopic changes to a high-spin→low-spin transition of heme b_{595}. However, the current work reveals a number of factors complicating the previous interpretation of the data, requiring revision of this interpretation.

First, our earlier experiments had been performed with the solubilized, purified enzyme. It has since been determined that solubilization of cytochrome by SB-12 (*N*-dodecyl-*N*,*N*-

dimethylammonio-3-propanesulfonate), which is the detergent used for purification of the enzyme (*67*), can destabilize the coordination sphere of heme b_{558} (I. Smirnova et al., unpublished). Hence, in cytochrome *bd* purified with this detergent, under some conditions, a fraction of the ferric heme b_{558} is in the high-spin state and reacts readily with CN^- even at low concentrations of the ligand. Some high-spin heme b_{558} was present in the preparations used in (*26*), and conversion of the high-spin fraction of b_{558} to the low-spin CN^- complex contributed significantly to the MCD changes observed in this earlier work.

Second, it is now evident that in the purified cytochrome *bd* complex (but not in membranes), even the "native" six-coordinate, low-spin ferric heme b_{558} interacts significantly with CN^- at high concentrations of the latter. The interaction of low-spin heme b_{558} with CN^- is perhaps not surprising since the heme iron in cytochrome b_{558} has His and Met as axial ligands, rather than the more usual case of two histidines as axial ligands (*61, 64*). Methionine is a relatively weak axial ligand for the ferric heme iron and can be displaced by strong exogenous ligands such as CN^-. For instance, ferric horse heart cytochrome *c* reacts with CN^- with an apparent K_d of ca. 2 mM (*81*). Therefore, attribution of CN^--induced MCD and absorption changes to high-spin b_{595} rather than to low-spin heme b_{558}, which was the most natural interpretation at the time of the earler publication (*26*), was not correct. Heme b_{558} contributes significantly to the MCD changes upon binding of CN^- to the enzyme.

Third, the studies in (*26, 40*) were carried out with the 'aerobically oxidized' (as isolated) form of the enzyme, in which heme *d* is predominantly in the oxygenated (ferrous heme *d*−oxy) state. Formation of the CN^- complex with ferric heme *d* under these conditions is accompanied by the displacement of dioxygen and intramolecular electron transfer from ferrous−oxy heme *d* to the hemes *b* (*48*). As found in (*66*), the presence of ferricyanide does not provide for efficient reoxidation of the reduced hemes *b*. Accordingly, it was suggested (*48*) that part of the CN^--induced spectroscopic changes described in (*26*) could be associated with reduction of heme b_{595} by the electron displaced from heme *d* upon CN^- binding. Tsubaki et al. [see footnote 3 in ref (*40*)] proposed a more radical idea that heme b_{558} is converted to a pentacoordinate high-spin form in the oxygenated cytochrome *bd*, thus drastically changing the ligand reactivity of the enzyme in this form of the enzyme.

In the present work, the complications described above have been taken into account. The better defined, fully oxidized form of cytochrome *bd*, rather than the 'as isolated' form of the enzyme, has been used as the initial state for CN^- binding. In addition, improved preparations of the enzyme (isolated from a different strain, GO105/pTK1) were used in which the amount of the high-spin form of cytochrome b_{558} was very small. With several such preparations tested, the interaction of CN^- with the *b*-type hemes is much less pronounced than previously observed in (*26*) [cf. Figure 8A in this paper and Figure 4 in ref (*26*)]. The minor interaction that is observed in the improved preparations is with the low-spin heme b_{558} rather than the high-spin heme b_{595}. Therefore, it is concluded that in the oxidized cytochrome *bd*, heme b_{595} does not interact with CN^-.

This is consistent with the lack of reaction of hydrogen peroxide with heme b_{595} in fully oxidized cytochrome *bd* (*78, 79*). Ferric heme b_{595} does not bind to exogenous ligands under the conditions examined.

Reduced Heme b_{595} Does Not React with CO or NO. It can also be concluded that in the fully reduced cytochrome *bd*, the major part of ferrous heme b_{595} does not react with either CO or NO, at room temperature. That a small fraction of the heme (<5%) can bind these ligands cannot be excluded, as discussed below in more detail. This conclusion accords with the finding that ferrous heme b_{595} does not bind CN^- (*42*), which is, however, less surprising since CN^- is a rather poor ligand for ferrous hemoproteins. On the other hand, there is a considerable body of evidence that "...has clearly shown that cytochrome b_{595} in both the *E. coli* and *A. vinelandii bd*-type oxidases also bind CO" (*19*) [and see also (*21*) for a more recent review]. The earlier conclusions concerning the interactions of ferrous heme b_{595} with CO and other ligands at room temperature deal with at least two different effects.

1. Low-Affinity CO Binding with Heme b_{595}. It was found in a number of earlier studies that while heme *d* absorption changes are saturated at low (several micromolar) concentrations of CO or NO, a further increase of ligand concentration results in a second phase of absorption changes that are clearly due to ligand binding with heme *b*. These secondary changes have been assigned as being due to low-affinity ligand binding with heme b_{595} [e.g., (*41*)].

Data reported in the current work are consistent with the previous results, but the new results suggest a different interpretation. It is clear from the MCD spectra that a major part of these secondary absorption changes induced by CO ("low-affinity binding") involving a blue shift in the Soret (derivative-shaped feature with a peak at 416 nm and a trough at 430 nm) and a trough around 560 nm is mostly due to binding of the ligand with low-spin heme b_{558}. CO binding to low-spin heme b_{558} is also indicated by the γ/α amplitude ratio of ca. 7 for these changes that is diagnostic of CO binding with the low-spin cytochrome *b* (*82*)

2. High-Affinity Binding of CO with Heme b_{595}. The spectroscopic responses of the reduced cytochrome *bd* to CO or NO appear heterogeneous, even at low ligand concentrations about equimolar to the enzyme. Heterogeneity is indicated by the rather complex line shapes of the difference absorption spectra induced by low concentrations of CO and NO in the Soret (the W-shaped trough with minima at 429−430 and 443−444 nm, e.g., see Figure 1) and by CO photodissociation studies [see (*18, 46*)]. Some workers have assigned the minimum at 429 nm in the CO-induced difference spectra to heme b_{595} (previously called cytochrome a_1) and the negative band at about 443 nm to heme *d* (*41, 83, 84*). In contrast, Poole attributes the trough at 443 nm to heme b_{595} (*18*). Importantly, the overall W-shaped difference spectrum titrates essentially in parallel with the well-resolved response of heme *d* in the near-IR region (*41*) (Smirnova et al., in preparation), and saturates upon the binding of about 1 mol of CO or NO per mole of cytochrome *bd* complex (*41*). It is necessary to explain how binding of one molecule of CO or NO can induce the putative spectroscopic response of heme b_{595}, in addition to the unambiguous effect on heme *d*.

It must be emphasized that whatever the attribution, the commonly observed ligand-induced changes in the Soret of the reduced cytochrome *bd* are very small, with an exception

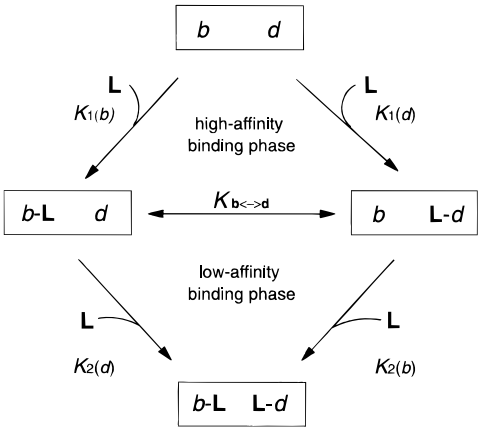

FIGURE 9: Scheme for ligand binding to the high-spin hemes b_{595} and *d* of cytochrome *bd*. The model presumes that the two hemes share a binding pocket within the protein. It is proposed that the intrinsic ligand affinity to heme *d* is substantially greater than for heme b_{595} ($K_{d\leftrightarrow b} \ll 1$) and that there is strong negative cooperativity that disfavors two ligands bound simultaneously.

of the effects of high NO concentrations after very prolonged incubation [cf. Figure 4 in ref. (*44*)]. The magnitude of the changes observed at either 431 or 444 nm is typically 5−10 mM^{-1} cm^{-1} (e.g., Figure 1), which can be compared to a $\Delta\epsilon_{max-min}$ value of about 150−200 mM^{-1} cm^{-1} for the typical CO-induced difference spectrum of a ferrous high-spin *b*-type hemoprotein (*82*). Therefore, the CO- and NO-induced responses observed with cytochrome *bd* are likely to correspond to no more than 5% of heme b_{595} interacting with the ligand. There are two alternative interpretations of the small magnitude of these changes.

First, it is possible that the effect is due to a small fraction of the population having a highly ligand-reactive heme *b*. Contribution from a high-spin heme b_{558} often present in purified preparations of the enzyme cannot be excluded. However, the CO-induced difference spectra of the membrane-bound cytochrome *bd* are less likely to be explained that way. A possible origin of the small, highly CO-reactive fraction of heme b_{595} in the intact preparations is considered below (see Figure 9). Nevertheless, the major point remains that if the response is due to direct ligand interaction with one of the heme *b* components of the enzyme, it must represent a very small portion of the population.

An alternative explanation is that the small spectroscopic changes observed are an indirect effect on the spectrum of heme b_{595} due to ligand binding to heme *d*. The perturbation of the absolute spectrum of heme b_{595}, in this case, should be much smaller than expected for direct ligation to the heme iron, and, thus, the modest size of the absorption changes can report a minute response in the entire population of heme b_{595}. Such a proposal rationalizes the parallel titration of the "W-shaped" Soret response of cytochrome *bd* with the heme *d* changes in the far-red region in the high-affinity phase of ligand binding, as well as their parallel development in the rapid phase of CO recombination following flash-photolysis in cytochrome *bd* from *A. vinelandii* (*46*) and *E. coli* (Smirnova et al., in preparation).

Why Heme b_{595} Does Not Interact with Ligands: An Anticooperativity Model. Whatever the origin of the small CO-induced absorption changes of heme b_{595}, the data show that the major part of this redox center does not bind ligands in either the reduced or the oxidized state. Resistance of a pentacoordinated high-spin hemoprotein to interaction with small exogenous ligands such as CO, CN^-, or H_2O_2 is very unusual. A model that can account for such an unusual behavior was proposed earlier (*78*) and is based on the following three postulates.

(1) Both high-spin hemes b_{595} and *d* can bind exogenous ligands.

(2) There is strong negative cooperativity between ligand binding to hemes *d* and b_{595}. If a ligand coordinates to one of the hemes, b_{595} or *d*, the second molecule of ligand cannot bind to the second heme due to either a thermodynamic (decreased affinity) or a kinetic effect (blocked access). The first of these possibilities (thermodynamic) is illustrated by the scheme in Figure 9. A simple mechanism for such a negative cooperativity might consist in the proximity of the two heme irons, so that only one ligand molecule can squeeze into the heme pocket.

(3) The intrinsic affinity of heme *d* for the ligands is much higher than that of heme b_{595} ($K_{b\leftrightarrow d} \ll 1$ in the scheme in Figure 9; $K_{b\leftrightarrow d}$ is the equilibrium constant for the ligand distribution between hemes b_{595} and *d*).

As a consequence of these three postulates, the thermodynamically stable complex of cytochrome *bd* with ligands at low concentrations of the latter ([L] < K_2) will correspond to a state with one molecule of the ligand bound to the enzyme and located mostly at the heme *d* iron site.

This model leads to a reasonable interpretation of many of the data available on the ligand reactivity of cytochrome *bd*, and allows one to make some testable predictions.

Room-Temperature Studies. If the anticooperative interactions between hemes b_{595} and *d* are thermodynamic (Figure 9), the model predicts that CO^-- or NO-induced spectroscopic changes of both hemes b_{595} and *d* should reveal a second low-affinity phase. Given $K_{b\leftrightarrow d}$ is ≪1, the amplitude of the heme *d* spectroscopic changes in this second phase is expected to be small (as most of the heme will bind the ligand in the high-affinity phase) and would easily go unnoticed. However, the low-affinity phase of heme b_{595} has to be a major process and should be visible provided one can go to high enough concentrations of the ligand.

As discussed above, the "low affinity" CO binding with *b*-type heme, manifested as the 415/431 nm derivative-shaped curve in the Soret and a trough at 560 nm with a Soret to α amplitude ratio of ca. 7 (*41*, *85*), appears to be reporting CO interaction with the low-spin heme b_{558}, as evidenced by the MCD studies. Therefore, reference to these data as indicating "low affinity ligand binding by heme b_{595}" (*21*, *41*) is probably incorrect.

However, in addition to these changes of low-spin heme b_{558}, the difference spectra between the effects of high and low concentrations of CO show consistently some growth of the trough at 443 nm (Figure 1, spectrum 3). The 443 nm trough is not accompanied by additional changes in the visible and near-IR bands of heme *d*. This phenomenon could be due to the predicted second phase of CO binding with heme b_{595} with low affinity (Figure 9), and is also consistent with attribution of the 443 nm trough to heme b_{595} (*18*) rather than to heme *d* (*21*, *41*). It is of critical importance to establish unambiguously whether the growth of the trough at 443 nm at high CO concentrations is paralleled by the changes around ca. 590 nm in the visible. Spectroscopic

changes at high CO pressure give clear evidence for a shift of the 590 nm band in the purified cytochrome *bd* from *E. coli* (Smirnova et al., in preparation). Absorption changes in the 590−600 nm range induced by high concentrations of CO and especially NO have also been reported for the *A. vinelandii* cytochrome *bd* (*41*). Quantitation of the heme−nitrosyl EPR signals in *A. vinelandii* (*41*) and *E. coli* (*44*) indicates possible binding of 2 equiv of NO to reduced cytochrome *bd* at 1 mM of the ligand, whereas at micromolar concentrations of NO only 1 equiv of NO is bound.

The model in Figure 9 also provides a simple explanation as to why cytochromes *bd* from different species show somewhat different line shapes of the CO-induced absorption changes. For example, in *A. vinelandii* (*41*), *Bacillus subtilis* (*77*), and *Klebsiella pneumoniae* (*9*), the troughs at about 600 nm in the visible and at 443 nm in the Soret band induced by CO are more pronounced as compared to *E. coli*. Different equilibrium constants, $K_{b\leftrightarrow d}$, of the ligand distribution between hemes *d* and b_{595} in the singly CO-ligated state (Figure 9) could account for these observations.

In sum, the data favor the model of anticooperative interactions between heme *d* and heme b_{595}. The small indirect spectral shift of heme b_{595} induced by ligation of CO/NO to heme *d* is very likely, but it is more difficult to reconcile with these data as the only factor. However, a combination of the both effects, i.e., perturbation of the spectrum of heme b_{595} induced by ligand binding to heme *d* plus some binding of the ligand directly to heme b_{595} according to the Figure 9, could well be the case.

Low-Temperature Studies. Whereas the analysis of the data obtained at room temperature argues against significant ligand interaction with heme b_{595}, the low-temperature photodissociation experiments of Poole and co-workers [see (*24*, *45*) and references to the earlier works of the group therein] and those in (*25*) provide strong evidence for CO binding with a very significant fraction of heme b_{595} in the reduced membrane-bound form of cytochrome *bd*. The discrepancy between the experiments done at room and cryogenic temperatures can also be explained provisionally by the anticooperative model in Figure 9, assuming that the relative affinity of CO binding to heme b_{595} is increased in the frozen samples.

In the experiments of Hill et al. (*25*), FTIR spectroscopy was used to monitor the redistribution of CO between hemes b_{595} and *d* at liquid helium temperatures. The spectroscopy showed that (1) freezing was rapid enough to trap the enzymes in the room-temperature state with CO bound essentially to heme *d*; (2) following photodissociation of CO from heme *d* into the heme pocket, the ligand was able to bind heme b_{595} in at least 5−15% of the cytochrome; moreover, very slow spontaneous transfer of CO from heme *d* to heme b_{595} in the dark could be observed (J. Hill and R. B. Gennis, unpublished). These data are fully consistent with Figure 9, assuming that at low temperatures the binding of CO to heme b_{595} becomes more favorable thermodynamically, but that there is a very significant barrier for equilibration of the ligand between the two hemes in the frozen matrix at liquid helium temperatures.

CO photodissociation from heme b_{595} in the frozen samples at higher temperatures (ca., −100 °C), as revealed by absorption spectroscopy in the experiments of Poole's group, can also be explained by a temperature- or freezing-dependent shift in $K_{b\leftrightarrow d}$ in Figure 9 in favor of heme b_{595}. In this case, it is, however, necessary to assume either (i) that freezing was relatively slow so as to allow for dark reequilibration of the ligand between the heme groups or (ii) that at temperatures as high as −100 °C, dark equilibration can be fast enough even in the frozen matrix, as opposed to liquid helium temperatures in (*25*). What is now evident, however, is a discrepancy between the results of CO-binding studies performed at room temperature and those done with the frozen samples. Additional and more systematic experiments performed over a wider range of cryogenic temperatures will be required to obtain a fully consistent picture and resolve the discrepancy. It also needs to be determined whether the method and/or rate of freezing of the samples might play a crucial role, determining the distribution of CO between hemes b_{595} and *d* prior to photodissociation.

ACKNOWLEDGMENT

We are indebted to Dr. N. Segal for her assistance in the experiments with NO.

REFERENCES

1. Saraste, M., Holm, L., Lemieux, L., Lubben, M., and van der Oost, J. (1991) *Biochem. Soc. Trans. 19*, 608−612.
2. Garcia-Horsman, J. A., Barquera, B., Rumbley, J., Ma, J., and Gennis, R. B. (1994) *J. Bacteriol. 176*, 5587−5600.
3. Saraste, M., and Castresana, J. (1994) *FEBS Lett. 341*, 1−4.
4. Saraste, M., Castresana, J., Higgins, D., and Lübben, M. (1994) in *Origin and Evolution of Biological Energy Conversion* (Baltscheffsky, H., Ed.) VCH, New York (in press).
5. Purschke, G. W., Schmidt, C. L., Petrsen, A., and Schafer, G. (1997) *J. Bacteriol. 179*, 1344−1353.
6. Mattar, S., and Engelhard, M. (1997) *Eur. J. Biochem. 250*, 332−341.
7. Kelly, M. J. S., Poole, R. K., Yates, M. G., and Kennedy, C. (1990) *J. Bacteriol. 172*, 6010−6019.
8. Hill, S., Viollet, S., Smith, A. T., and Anthony, C. (1990) *J. Bacteriol. 172*, 2071−2078.
9. Smith, A., Hill, S., and Anthony, C. (1990) *J. Gen. Microbiol. 136*, 171−180.
10. D′Mello, R., Hill, S., and Poole, R. K. (1994) *Microbiology 140*, 1395−1402.
11. Kaminski, P. A., Kitts, C. L., Zimmerman, Z., and Ludwig, R. A. (1996) *J. Bacteriol. 178*, 5989−5994.
12. Poole, R. K., and Hill, S. (1997) *Biosci. Rep. 17*, 307−317.
13. Henry, M. F. (1981) in *Cyanide in Biology* (Vennesland, B., Conn, E. E., Knowles, C. J., Westley, J., & Wissing, F., Eds.) pp 415−436, Academic Press, London.
14. Miller, M. J., and Gennis, R. B. (1985) *J. Biol. Chem. 260*, 14003−14008.
15. Puustinen, A., Finel, M., Haltia, T., Gennis, R. B., and Wikström, M. (1991) *Biochemistry 30*, 3936−3942.
16. Bertsova, Y. V., Bogachev, A. V., and Skulachev, V. P. (1997) *FEBS Lett. 414*, 369−372.
17. Kolonay, J. F., Jr., and Maier, R. J. (1997) *J. Bacteriol. 179*, 3813−3817.
18. Poole, R. K. (1988) in *Bacterial Energy Transduction* (Anthony, C., Ed.) pp 231−291, Academic Press, London.
19. Poole, R. K. (1994) *Antonie van Leeuwenhoek 65*, 289−310.
20. Borisov, V. B. (1996) *Biochemistry (Moscow) 61*, 565−574.
21. Jünemann, S. (1997) *Biochim. Biophys. Acta 1321*, 107−127.
22. Poole, R. K., and Williams, H. D. (1987) *FEBS Lett. 217*, 49−52.
23. Rothery, R. A., Houston, A. M., and Ingledew, W. J. (1987) *J. Gen. Microbiol. 133*, 3247−3255.
24. D'Mello, R., Hill, S., and Poole, R. K. (1996) *Microbiology 142*, 755−763.

25. Hill, J. J., Alben, J. O., and Gennis, R. B. (1993) *Proc. Natl. Acad. Sci. U.S.A. 90*, 5863−5867.
26. Krasnoselskaya, I., Arutjunjan, A. M., Smirnova, I., Gennis, R., and Konstantinov, A. A. (1993) *FEBS Lett. 327*, 279−283.
27. Poole, R. K., Waring, A. J., and Chance, B. (1979) *Biochem. J. 184*, 379−389.
28. Poole, R. K., and Chance, B. (1981) *J. Gen. Microbiol. 126*, 277−287.
29. Poole, R. K., Baines, B. S., Hubbard, J. A. M., Hughes, M. N., and Campbell, N. J. (1982) *FEBS Lett. 150*, 147−150.
30. Poole, R. K., Kumar, C., Salmon, I., and Chance, B. (1983) *J. Gen. Microbiol. 129*, 1335−1344.
31. Kahlow, M. A., Zuberi, T. M., Gennis, R. B., and Loehr, T. M. (1991) *Biochemistry 30*, 11485−11489.
32. Kahlow, M. A., Loehr, T. M., Zuberi, T. M., and Gennis, R. B. (1993) *J. Am. Chem. Soc. 115*, 5845−5846.
33. Hill, B. C., Hill, J. J., and Gennis, R. B. (1994) *Biochemistry 33*, 15110−15115.
34. Wikström, M., Krab, K., and Saraste, M. (1981) *Cytochrome Oxidase*—*A Synthesis*, Academic Press, New York.
35. Babcock, G. T., and Wikström, M. (1992) *Nature 356*, 301−309.
36. Mitchell, P. (1988) *Ann. N.Y. Acad. Sci. 550*, 185−198.
37. Morgan, J. E., Verkhovsky, M. I., and Wikström, M. (1994) *J. Bioenerg. Biomembr. 26*, 599−608.
38. Lorence, R. M., Miller, M. J., Borochov, A., Faiman-Weinberg, R., and Gennis, R. B. (1984) *Biochim. Biophys. Acta 790*, 148−153.
39. Jünemann, S., Butterworth, P. J., and Wrigglesworth, J. M. (1995) *Biochemistry 34*, 14861−14867.
40. Tsubaki, M., Hori, H., Mogi, T., and Anraku, Y. (1995) *J. Biol. Chem. 270*, 28565−28569.
41. Jünemann, S., and Wrigglesworth, J. M. (1995) *J. Biol. Chem. 270*, 16213−16220.
42. Sun, J., Kahlow, M. A., Kaysser, T. M., Osborne, J. P., Hill, J. J., Rohlfs, R. J., Hille, R., Gennis, R. B., and Loehr, T. M. (1996) *Biochemistry 35*, 2403−2412.
43. Koland, J. G., Miller, M. J., and Gennis, R. B. (1984) *Biochemistry 23*, 1051−1056.
44. Hori, H., Tsubaki, M., Mogi, T., and Anraku, Y. (1996) *J. Biol. Chem. 271*, 9254−9258.
45. D'Mello, R., Palmer, S., Hill, S., and Poole, R. K. (1994) *FEMS Microbiol. Lett. 121*, 115−120.
46. Jünemann, S., Rich, P. R., and Wrigglesworth, J. M. (1995) *Biochem. Soc. Trans. 23*, 157S.
47. Jünemann, S., and Wrigglesworth, J. M. (1996) *Biochem. Soc. Trans. 24*, 38S.
48. Sun, J., Osborne, J. P., Kahlow, M. A., Kaysser, T. M., Gennis, R. B., and Loehr, T. M. (1995) *Biochemistry 34*, 12144−12151.
49. Lorence, R. M., Koland, J. G., and Gennis, R. B. (1986) *Biochemistry 25*, 2314−2321.
50. Sharonov, Y. A. (1991) in *Soviet Scientific Reviews/Section D: Physicochemical Biology Reviews* (Skulachev, V. P., Ed.) pp 1−118, Harwood Academic Publishers, Newark, NJ.
51. Cheesman, M. R., Greenwood, C., and Thomson, A. J. (1991) *Adv. Inorg. Chem. 36*, 201−255.
52. Arutjunjan, A. M., Konstantinov, A. A., and Sharonov, Y. A. (1974) *FEBS Lett. 46*, 40−44.
53. Carithers, R. P., and Palmer, G. (1981) *J. Biol. Chem. 256*, 7967−7976.
54. Eglinton, D. G., Johnson, M. K., Thomson, A. J., Gooding, P. E., and Greenwood, C. (1980) *Biochem. J. 191*, 319−331.
55. Thomson, A. J., Johnson, M. K., Greenwood, C., and Gooding, P. E. (1981) *Biochem. J. 193*, 687−697.
56. Thomson, A. J., Englinton, D. G., Hill, B. C., and Greenwood, C. (1982) *Biochem. J. 207*, 167−170.
57. Thomson, A. J., Greenwood, C., Gadsby, P. M. A., Peterson, J., Eglinton, D. G., Hill, B. C., and Nicholls, P. (1985) *J. Inorg. Biochem. 23*, 187−197.
58. Cheesman, M. R., Watmough, N. J., Pires, C. A., Turner, R., Brittain, T., Gennis, R. B., Greenwood, C., and Thomson, A. J. (1993) *Biochem. J. 289*, 709−718.
59. Cheesman, M. R., Watmough, N. J., Gennis, R. B., Greenwood, C., and Thomson, A. J. (1994) *Eur. J. Biochem. 219*, 595−602.
60. Watmough, N. J., Cheesman, M. R., Gennis, R. B., Greenwood, C., and Thomson, A. J. (1993) *FEBS Lett. 319*, 151−154.
61. Spinner, F., Cheesman, M. R., Thomson, A. J., Kaysser, T., Gennis, R. B., Peng, Q., and Peterson, J. (1995) *Biochem. J. 308*, 641−644.
62. Borisov, V. B., Osborne, J. P., Arutjunjan, A. M., Smirnova, I. A., Gennis, R. B., and Konstantinov, A. A. (1996) *EBEC Short Rep. 9*, 80.
63. Borisov, V. B., Osborne, J. P., Arutjunjan, A. M., Gennis, R. B., and Konstantinov, A. A. (1998) *EBEC Short Rep. 10*, 85.
64. Kaysser, T. M., Ghaim, J. B., Georgiou, C., and Gennis, R. B. (1995) *Biochemistry 34*, 13491−13501.
65. Miller, M. J., and Gennis, R. B. (1986) *Methods Enzymol. 126*, 138−145.
66. Borisov, V. B., Smirnova, I. A., Krasnosel'skaya, I. A., and Konstantinov, A. A. (1994) *Biochemistry (Moscow) 59*, 437−443.
67. Miller, M. J., and Gennis, R. B. (1983) *J. Biol. Chem. 258*, 9159−9165.
68. Kita, K., Konishi, K., and Anraku, Y. (1984) *J. Biol. Chem. 259*, 3375−3381.
69. Nozawa, T., Kobayashi, N., and Hatano, M. (1976) *Biochim. Biophys. Acta 427*, 632−662.
70. Vickery, L., Nozawa, T., and Sauer, K. (1976) *J. Am. Chem. Soc. 98*, 351−357.
71. Vickery, L., Salmon, A., and Sauer, K. (1975) *Biochim. Biophys. Acta 386*, 87−98.
72. Sutherland, J. C., and Klein, M. P. (1972) *J. Chem. Phys. 57*, 76−86.
73. Zickermann, I., Tautu, O. S., Link, T. A., Korn. M., Ludwig. B., and Richter, O.-M. H. (1997) *Eur. J. Biochem. 246*, 618−624.
74. Vickery, L., Nozawa, T., and Sauer, K. (1976) *J. Am. Chem. Soc. 98*, 343−350.
75. Bracete, A. M., Kadkhodayan, S., Sono, M., Huff, A. M., Zhuang, C., Cooper, D. K., Smith, K. S., Chang, C. K., and Dawson, J. H. (1994) *Inorg. Chem. 33*, 5042−5049.
76. Huff, A. M., Chang, C. K., Cooper, D. K., Smith, K. M., and Dawson, J. H. (1993) *Inorg. Chem. 32*, 1460−1466.
77. Azarkina, N., Borisov, V. N., and Konstantinov, A. (1997) *FEBS Lett. 416*, 171−174.
78. Borisov, V. B., Gennis, R. B., and Konstantinov, A. A. (1995) *Biochemistry (Moscow) 60*, 231−239.
79. Borisov, V., Gennis, R., and Konstantinov, A. A. (1995) *Biochem. Mol. Biol. Int. 37*, 975−982.
80. Sono, M., Braceate, A. M., Huff, A. M., Ikeda-Saito, M., and Dawson, J. H. (1991) *Proc. Natl. Acad. Sci. U.S.A. 88*, 11148−11152.
81. George, P., and Tsou, C. L. (1952) *Biochem. J. 50*, 440−448.
82. Wood, P. M. (1984) *Biochim. Biophys. Acta 768*, 293−317.
83. Kauffman, H. F., van Gelder, B. F., and DerVartanian, D. V. (1980) *J. Bioenerg. Biomembr. 12*, 265−276.
84. Jünemann, S., Wrigglesworth, J. M., and Rich, P. R. (1997) *Biochemistry 36*, 9323−9331.
85. Jünemann, S., and Wrigglesworth, J. M. (1993) *Biochem. Soc. Trans. 21*, 345S.

BI981908T